

Wenjing Sun, Daniel Smith, Yan Fu, Ji-Xin Cheng, Steven Bryn, Richard Borgens and Riya Shi

J Neurophysiol 103:469-478, 2010. First published Nov 18, 2009; doi:10.1152/jn.00154.2009

You might find this additional information useful...

This article cites 52 articles, 10 of which you can access free at:

<http://jn.physiology.org/cgi/content/full/103/1/469#BIBL>

Updated information and services including high-resolution figures, can be found at:

<http://jn.physiology.org/cgi/content/full/103/1/469>

Additional material and information about *Journal of Neurophysiology* can be found at:

<http://www.the-aps.org/publications/jn>

This information is current as of January 18, 2010 .

Novel Potassium Channel Blocker, 4-AP-3-MeOH, Inhibits Fast Potassium Channels and Restores Axonal Conduction in Injured Guinea Pig Spinal Cord White Matter

Wenjing Sun,¹ Daniel Smith,³ Yan Fu,² Ji-Xin Cheng,² Steven Bryn,³ Richard Borgens,^{1,2} and Riya Shi^{1,2}

¹Department of Basic Medical Sciences, Center for Paralysis Research; ²Weldon School of Biomedical Engineering; and ³Department of Industrial and Physical Pharmacy, Purdue University, West Lafayette, Indiana

Submitted 5 March 2009; accepted in final form 9 November 2009

Sun W, Smith D, Fu Y, Cheng JX, Bryn S, Borgens R, Shi R. Novel potassium channel blocker, 4-AP-3-MeOH, inhibits fast potassium channels and restores axonal conduction in injured guinea pig spinal cord white matter. *J Neurophysiol* 103: 469–478, 2010. First published November 18, 2009; doi:10.1152/jn.00154.2009. We have demonstrated that 4-aminopyridine-3-methanol (4-AP-3-MeOH), a 4-aminopyridine derivative, significantly restores axonal conduction in stretched spinal cord white-matter strips and shows no preference in restoring large and small axons. This compound is 10 times more potent when compared with 4-AP and other derivatives in restoring axonal conduction. Unlike 4-AP, 4-AP-3-MeOH can restore axonal conduction without changing axonal electrophysiological properties. In addition, we also have confirmed that 4-AP-3-MeOH is indeed an effective blocker of I_A based on patch-clamp studies using guinea pig dorsal root ganglia cells. Furthermore, we have also provided the critical evidence to confirm the unmasking of potassium channels following mechanical injury. Taken together, our data further supports and implicates the role of potassium channels in conduction loss and its therapeutic value as an effective target for intervention to restore function in spinal cord trauma. Furthermore, due to its high potency and possible low side effect of impacting electrophysiological properties, 4-AP-3-MeOH is perhaps the optimal choice in reversing conduction block in spinal cord injury compared with other derivatives previously reported from this group.

INTRODUCTION

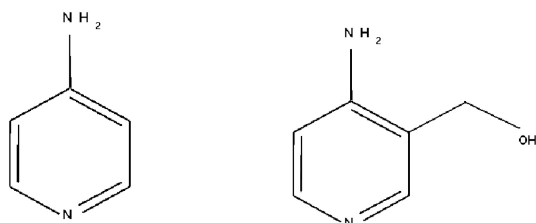
Traumatic spinal cord injury (SCI) results in severe functional deficits that are mainly due to damage in white matter. In most cases, axons are not completely severed but rather contused and/or compressed after SCI (Blight 1983a,b; Blight and DeCrescito 1986; Hayes and Kakulas 1997; Kakulas 1999). These anatomically continuous but functionally silent axons offer a realistic opportunity for functional restoration through therapeutic interventions. It is well accepted that myelin damage, a well-known pathology in SCI, could expose the fast potassium channels that directly contribute to conduction failure (Blight 1989; Blight and Gruner 1987; Shi et al. 1997; Waxman 1992, 1994). Specifically, activated potassium channels allow leakage of positive charges carried by potassium during depolarization and prevent the initiation of an action potential. Therefore blocking such potassium channels has been identified as an effective means to restore axonal conduction (Blight et al. 1991; Hansebout et al. 1993; Shi et al. 1997; Waxman 1989).

For the last two decades, researchers have identified 4-aminopyridine (4-AP), a known fast potassium channel blocker, as an effective agent in restoring axonal conduction in traumatically injured spinal cord both in laboratory settings and in clinical applications (Blight 1989; Fujihara and Miyoshi 1998; Haghghi et al. 1995; Hayes et al. 1993, 1994; Jensen and Shi 2003; Jones et al. 1983; Stefoski et al. 1987). However, despite its effectiveness, the overall benefit resulting from 4-AP treatments remained modest. The main reason is that the achievable concentration of 4-AP in vivo is two orders of magnitude below its maximal effective dosage seen in vitro due to severe side effects seen in higher concentrations in live animals and human (Blight et al. 1991; Donovan et al. 2000; Halter et al. 2000). The common side effects include respiratory distress, anxiety, and epileptiform seizures (Pena and Tapia 1999, 2000; Stork and Hoffman 1994). Therefore alternative blockers that target the same channel but perhaps with greater efficacy and fewer side effects are highly desirable and warranted.

To pursue such a goal, we have in the last few years successfully synthesized three 4-AP derivatives that can significantly enhance axonal conduction following spinal cord trauma (McBride et al. 2006, 2007; Smith et al. 2005; Sun et al. 2009). More importantly, it was demonstrated that axons rescued by 4-AP derivatives can conduct action potentials in a manner that resembles normal axons more than those rescued by 4-AP (McBride et al. 2007). The minimal effective dosage of these 4-AP derivatives, however, is similar to that of 4-AP (at 1 μ M) which signifies the similar potency between 4-AP and its derivatives at the achievable level in vivo (McBride et al. 2006).

To continue this line of experimentation, we now report a new and fourth blocker in this series, 4-aminopyridine-3-methanol (4-AP-3-MeOH; Fig. 1). This compound can significantly enhance axonal conduction following mechanical trauma. Similar to the previous three carbamates, 4-AP-3-MeOH also restores conduction of injured axons in a manner similar to normal uninjured axons (McBride et al. 2007). However, a unique feature of 4-AP-3-MeOH is its high potency: the lowest effective dosage is 0.1 μ M, which is one order of magnitude lower than 4-AP and its derivatives (Jensen and Shi 2003; McBride et al. 2006; Shi and Blight 1997; Shi et al. 1997). In addition, we have found that 4-AP-3-MeOH is indeed capable of blocking fast potassium channels, which is likely responsible for restoring axonal conduction. We have also confirmed that potassium channels are indeed exposed following mechanical stretch in the current study. This further

Address for reprint requests and other correspondence: R. Shi, Department of Basic Medical Sciences, Weldon School of Biomedical Engineering, Purdue University, West Lafayette, IN 47907 (E-mail: riya@purdue.edu).



4 - AP 4-aminopyridine-3-methanol

FIG. 1. Structure of 4-aminopyridine and 4-aminopyridine-3-methanol (4-AP-3-MeOH).

strengthens the notion that potassium channels are a key pathology in myelin damage that contribute to conduction block and an important therapeutical target to restore axonal conduction.

METHODS

Isolation of spinal cord

The adult female guinea pig (300–450 g) was anesthetized with a combination of ketamine (80 mg/kg), xylazine (12 mg/kg), and acepromazine (0.8 mg/kg). After anesthesia the guinea pig was perfused with oxygenated, cold Krebs' solution [containing (in mM) 124 NaCl, 2 KCl, 1.2 KH₂PO₄, 1.3 MgSO₄, 2 CaCl₂, 10 dextrose, 26 NaHCO₃, and 10 sodium ascorbate]. The vertebral column was extracted, and spinal cords were isolated as previously described (Shi and Blight 1996; Shi and Pryor 2000; Shi et al. 2000). The protocol was approved by Purdue University Animal Care and Usage Committee (PACUC).

Double sucrose gap recording

A double sucrose gap chamber was used for compound action potential (CAP) recording as previously described (Shi and Blight 1996; Shi and Borgens 1999; Shi and Whitebone 2006). A 4.5-cm-long spinal cord ventral white-matter strip was placed across the chamber. The central compartment was continuously perfused with oxygenated Krebs' solution. The side compartments of the chamber were filled with isotonic potassium chloride (120 mM). Sucrose solution (320 mM) was perfused in the gaps for isolation. The temperature was maintained at 37°C for the duration of recording by a line heater and temperature probe (Warner Instruments, Hamden, CT). A bridge amplifier (Neurodata Instruments, Delaware Water Gap, PA) was used for recording, and data analysis was performed using customized Labview software (National Instruments, Austin, TX). 4-AP-MeOH was dissolved in Krebs' solution and directly delivered to the spinal cord strip by circulating it into the central compartment. 4-AP-3-MeOH powder was purchased from Alfa Aesar (Ward Hill, MA). According to the MSDS provided by Alfa Aesar, the purity of 4-AP-3-MeOH is 100%. The MSDS sheet of 4-AP-3-MeOH could be obtained from <http://www.alfa.com/content/msds/USA/H50033.pdf>.

Stretch injury model

An injury device that has a constant stretch magnitude and falling speed was used to induce stretch injury in this study (Jensen and Shi 2003; McBride et al. 2007; Shi and Pryor 2002). A stretch rod was released and falling at a speed ~1.5 m/s to induce the stretch injury to the spinal cord strip. A flat raised stage with a central hole was built in the central compartment of the double sucrose chamber, and the stretch rod would fall through the hole. A nylon mesh was laid on top

of the chamber to stabilize the strip of spinal cord. The rod and nylon mesh were removed immediately from the spinal cord after injury (Jensen and Shi 2003; McBride et al. 2007; Shi and Pryor 2002).

Coherent anti-Stokes Raman scattering imaging and immunofluorescence

Coherent anti-Stokes Raman scattering (CARS) imaging was used to visualize the myelin sheath directly without any staining (Fu et al. 2007; Wang et al. 2005). For immunofluorescence imaging, a 1-cm post-injury segment was cut from the central injury site and fixed in 4% paraformaldehyde for 24 h and followed with cryoprotection (incubation in 20% glycerol and 2% paraformaldehyde in PBS at 4°C) for 48 h. The strip was then sectioned into smaller pieces (~50 μm) using an oscillating tissue slicer (OTS-4000, Electron Microscopy Sciences, Hatfield, PA). After that, sections were incubated in 5% bovine serum albumin (BSA) with 0.5% Triton X-100 in PBS (pH 7.4) for blocking for 1 h at the room temperature. After rinsing with PBS, the sections were then incubated in 1:100 diluted Rabbit raised anti-Kv 1.2 (Alomone Labs, Jerusalem, Israel; 1% BSA with 0.1% Triton X-100 in PBS) at 4°C for 24 h. After being rinsed three times in PBS for total 30 min, the sections were then incubated in goat anti rabbit IgG conjugated with 1:100 diluted FITC-goat anti-rabbit IgG (H+L) (Invitrogen, Carlsbad, CA; 1% BSA with 0.1% Triton X-100 in PBS) for 1 h at the room temperature. Control sections were incubated with the secondary antibody only. After rinsing three times in PBS for 30 min, the sections were imaged by a laser scanning confocal microscope (FV300/IX70, Olympus) with a 488-nm laser.

The nodal ratio is calculated as nodal length divided by axon diameter. The nodal length was defined as the distance between paranodal myelin with strong CARS contrasts at the two ends along the node, and the axon diameter was defined as the distance between paranodal myelin at two sides across the node (Fig. 10B).

Acute dissociation of guinea pig DRG cells

The guinea pig DRG cell dissociation process has been described in detail previously (Sun et al. 2009). Briefly, dorsal root ganglia are collected from all accessible segments of guinea pig vertebra and digested with trypsin (type I, 0.25 mg/ml, Sigma-Aldrich) and collagenase (type I, 0.5 mg/ml, Sigma-Aldrich) at 37°C for 30 min. The dissociated dorsal root ganglion cells were plated on poly-L-lysine (0.2 mg/ml, coating overnight, Sigma-Aldrich)-coated dishes. They were cultured in medium [containing 48.5% DMEM (Sigma-Aldrich), 48.5% F-12 Nutrient Mixture (Gibco), 2% horse serum (Sigma-Aldrich), and 1% penicillin-streptomycin solution (Sigma-Aldrich)] at 37°C (5%CO₂ balance air, for 2.5 h before recording).

Whole cell patch-clamp recording

Currents were recorded using the Axopatch 200B amplifier (Molecular Devices, Union City, CA). Borosilicate glass tubing (Sutter Instrument, Novato, CA) was pulled using P-97 horizontal puller (Sutter Instruments) to make a recording pipette with resistances at ~4 MΩ. Pipette solution included (in mM) 140 KCl, 1 MgCl₂, 5 EGTA, and 10 HEPES titrated to pH 7.4 with KOH. Bath solution included (in mM) 145 NaCl, 2 KCl, 1 MgCl₂, 0.03 CaCl₂, and 10 HEPES and 1 μM TTX titrated to pH 7.4 with NaOH. Holding potential was -70 mV. The currents were filtered at 1–5 kHz, and the data were acquired and analyzed with pCLAMP 9.2 software (Molecular Devices).

Isolation of voltage-gated potassium currents

Na⁺ currents were blocked by 1 μM tetrodotoxin (TTX) in bath solution, and Ca²⁺ currents and Ca²⁺-dependent potassium currents were suppressed with low Ca²⁺ concentration (0.03 mM) in bath

solution. There are mainly two voltage-gated potassium (K_v) currents on guinea pig DRG cells: a transient fast activating A-type current (I_A) and a slow sustained delayed rectifier type current (I_{dr}) (Xu et al. 2006). I_{dr} can be separated from the total potassium currents recorded from DRG cells using a traditional electrophysiological method that is widely used in previous studies reported in the literature (Everill et al. 1998; Tan et al. 2006). The total outward potassium currents (I_{total}) were acquired from a series of 400-ms voltage stimuli ranging from -50 to 40 mV with 10-mV steps. Before the step stimuli, the cell was held at -100 mV (hyperpolarization) instead of -70 mV for 2 s. When the membrane potential was held at -30 mV (depolarization) for 2 s before the step stimuli, the fast-activating component I_A stays in the inactivation phase during the 400-ms step stimuli, and all the collected potassium currents were slow delay rectified component I_{dr} . All currents were off-line leak subtracted. 4-AP (5 mM) and 5 mM 4-AP-3-MeOH were applied into the bath solution respectively. 4-AP and 4-AP-3-MeOH were both freshly made with bath solution before recording.

Statistic analysis

Paired *t*-test was used to compare dose responses of 4-AP-3-MeOH after stretch injury, inhibition of potassium currents by 4-AP and 4-AP-3-MeOH as well as some electrophysiological tests analysis. Student's *t*-test was applied to analyze nodal ratio elongation.

RESULTS

4-AP-3-MeOH enhances compound action potential propagation in stretch-injured spinal cord white matter

After the stabilization of CAP recorded using double sucrose gap (Shi and Blight 1996; Shi and Borgens 1999; Shi and Whitebone 2006), a stretch injury was applied that initially completely abolished CAP conduction (Jensen and Shi 2003). The CAP then steadily recovered to reach a plateau after an average of 45 min (Fig. 2). The average amplitude of recovered CAP is $\sim 21\%$ of original CAP before the injury. 4-AP-3-MeOH was then applied through Krebs' circulation in the central compartment of double sucrose gap chamber. On average, the 4-AP-3-MeOH was applied for 40–50 min followed by a period of wash at 30–40 min.

As demonstrated in Fig. 3, 4-AP-3-MeOH significantly increased CAP conduction in the following four concentration groups (Fig. 3): $0.1 \mu\text{M}$ ($12.73 \pm 3.2\%$, mean \pm SE; $P < 0.01$, $n = 7$), $1 \mu\text{M}$ ($11.27 \pm 4.2\%$, $P < 0.05$, $n = 6$), $10 \mu\text{M}$ ($13.35 \pm 5.9\%$, $P < 0.05$, $n = 11$) and $100 \mu\text{M}$ ($21.51 \pm 4.5\%$, $P < 0.01$, $n = 6$). CAP was not significantly increased at $0.01 \mu\text{M}$ ($6.44 \pm 3.8\%$, $P > 0.05$, $n = 5$) and 1 mM ($6.72 \pm 8.3\%$, $P > 0.05$, $n = 5$). Similar to 4-AP and other 4-AP derivatives, 4-AP-3-MeOH at 10 mM suppressed CAP conduction ($18.48 \pm 8.1\%$, $P > 0.05$, $n = 5$).

4-AP-3-MeOH has no significant effect on activation threshold

A range of stimulus voltages was employed to assess CAP activation threshold. Stimulus intensities from 1.85 to 6.5 V were applied to injured spinal cord tissue pre and post $100 \mu\text{M}$ 4-AP-3-MeOH treatment. It is clear that 4-AP-3-MeOH increased CAP conduction at all stimuli intensity levels (Fig. 4). In addition, the CAP amplitude-stimulus intensity curves were similar in pre and after 4-AP-3-MeOH treatment (Fig. 4B). Figure 4C demonstrated the linear correlation between pre-

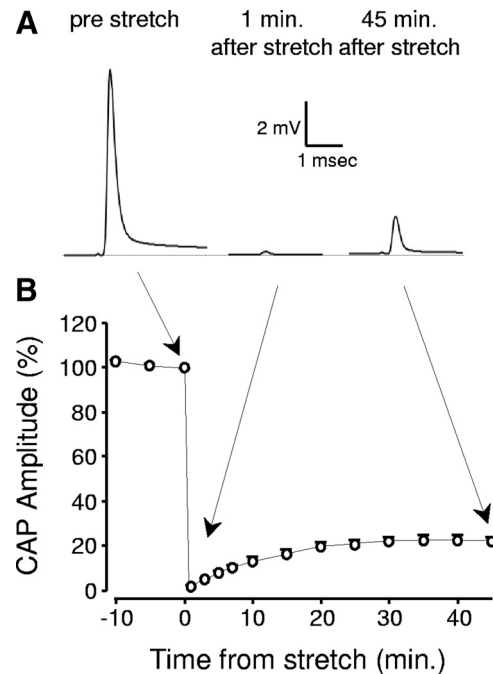


FIG. 2. Post injury self-recovery of compound action potential (CAP) conduction. A: representative CAP amplitude time history after stretch injury. B: histogram demonstrates that the CAP was abolished immediately after injury, but slowly recovered to a stable plateau at $21.75 \pm 2.3\%$ ($n = 12$) after 45 min. The CAP amplitude before stretch was normalized to 100%. Error bars denote SE.

drug amplitude (%max) and 4-AP-3-MeOH treated amplitude (%max). The slope of curve 1 indicates that 4-AP-3-MeOH induced conduction enhancement was not biased toward axons with different thresholds for activation.

4-AP-3-MeOH has no significant effect on axonal response to dual and multiple stimuli

To detect the effect of 4-AP-3-MeOH on spinal cord's response to multiple stimuli, we measured the refractory period and the response to train stimulus, respectively. For refractory period, spinal cord tissue was stimulated by dual stimuli with various interval times, ranging from 0.5 to 15 ms. Absolute refractory period (interval time that second peak starts to appear) and relative refractory period (interval time that 2nd peak amplitude is no $< 95\%$ of the 1st peak) were determined. It is demonstrated that 4-AP-3-MeOH at $100 \mu\text{M}$ has little effect on both absolute and relative refractory periods of injured spinal cord tissue ($P > 0.05$, Fig. 5).

We also measured the response of injured spinal cord in response to multiple (or train) stimuli after 4-AP-3-MeOH administration. A train stimulus at the duration of 100 ms with high and low frequency (1,000 and 500 Hz, respectively) was applied to the injured spinal cord strip. The representative CAP response is shown in Fig. 6A. The CAP response is quantified by averaging the last four CAP peaks as the percentage of first peak. Figure 6B demonstrates the comparison of CAP responses in pre-drug and drug conditions. The CAP response following train stimuli (both high and low frequency) is not significantly affected by application of 4-AP-3-MeOH ($P > 0.05$ in comparisons of pre-drug and drug, 1,000 and 500 Hz).

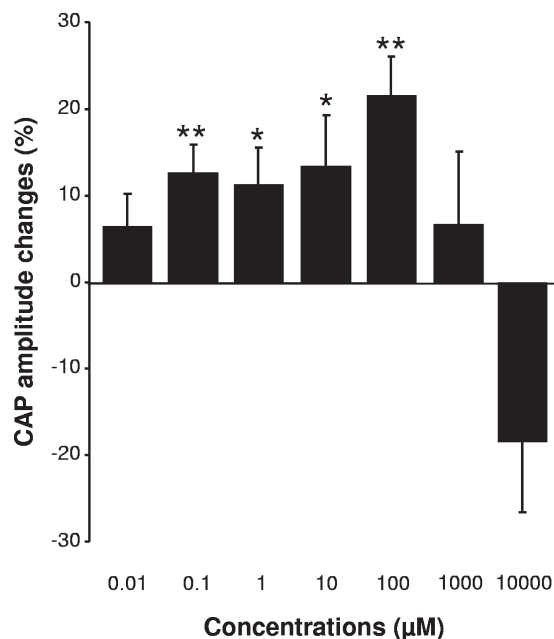


FIG. 3. The change of CAP amplitude in injured spinal cord tissue in response to various concentrations of 4-AP-3-MeOH. The 4-AP-3-MeOH was applied after 30–40 min after injury and recovery. The increase in CAP amplitude as a result of 4-AP-3MeOH was normalized to the pre-4-AP-3MeOH level. CAP amplitude significantly increased in 4 concentration groups (from 0.1 to 100 μ M). 4-AP-3-MeOH at 1 mM did not significantly enhance CAP amplitude ($6.72 \pm 8.3\%$, $n = 5$, $P > 0.05$). At 10 mM, 4-AP-3-MeOH began to show toxic effects ($-18.48 \pm 8.1\%$, $n = 5$, $P > 0.05$). All concentration groups were compared with control with a paired t -test. Error bars represent SE. * $P < 0.05$, ** $P < 0.01$.

4-AP-3-MeOH blocks fast potassium channels in guinea pig DRG neurons

Following the assertion that 4-AP-3-MeOH enhances CAP conduction in injured spinal cord, we investigated whether 4-AP-3-MeOH indeed block fast outward potassium currents as speculated. This was carried out using a patch-clamp technique (whole cell patch configuration) on guinea pig DRG cells where fast potassium currents are known to exist (Xu et al. 2006). Figure 7A shows the total voltage-gated potassium currents (I_{total}) recorded from guinea pig DRG cells elicited with a series of 400-ms step pulses. With a 2-s prepulse hyperpolarizing holding potential (-100 mV), the potassium currents are activated to a peak (transient) and then partially decayed to a sustained level. There are two significant and distinguishable components contributing to this current: one is fast activated and fast inactivated current called I_A , represented by the transient peak in the I_{total} ; the other component, delay rectifier, I_{dr} , is relatively slowly activated but sustained during the step pulse duration (Stewart et al. 2003; Tan et al. 2006; Xu et al. 2006).

When we applied 5 mM 4-AP through the bath solution, we found the initial peak was largely blocked while the sustained delayed rectifier component remained relatively unchanged (Fig. 7B). 4-AP-sensitive potassium current is shown in Fig. 7C by subtracting the current after treatment from pretreatment (A and B). Quantification analysis of drug effect was carried out at a particular command potential of +30 mV (Fig. 7D). When compared at the initial peak current (which is largely I_A), the I_{total} amplitude decreased from $4,306.38 \pm 810.2$ pA

(peak value) to $2,574.91 \pm 446.8$ pA as a result of 4-AP application (Fig. 7, D and E, $P < 0.05$, $n = 6$, paired t -test). This has confirmed the existence of 4-AP-sensitive I_A .

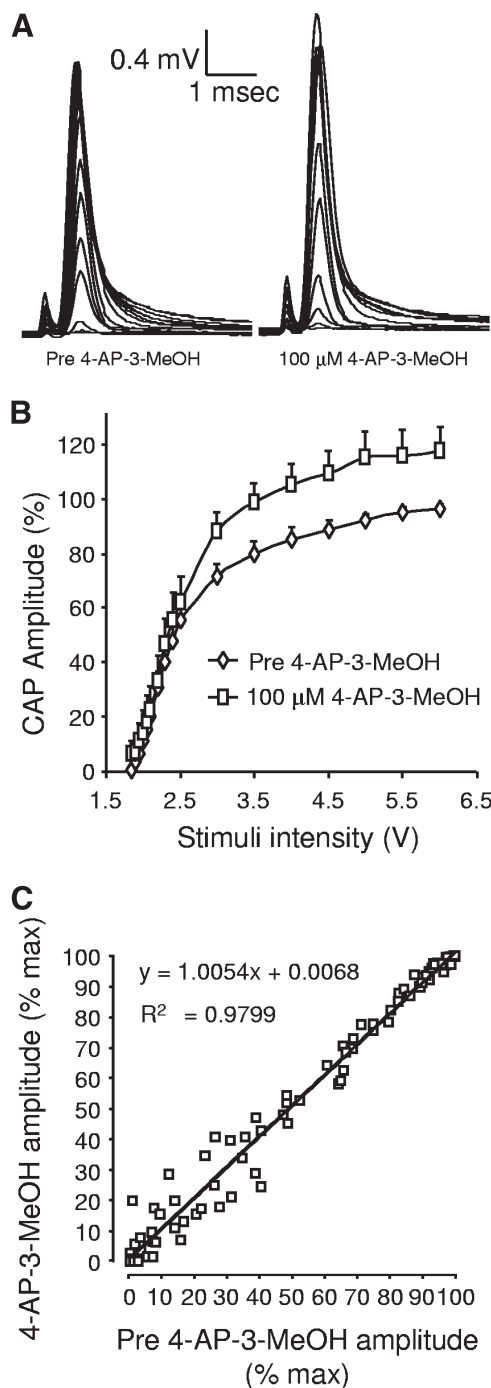


FIG. 4. A voltage test was performed to chart CAP responses (stretched cord) at different stimulus intensities and at 2 conditions: pre-drug and 100 μ M 4-AP-3MeOH-treated. CAP responses were shown in both superimposed form (A) and graphic plot form (B). Stimulus intensities ranged from 1.85 to 6.5 V, $n = 5$. Normalized CAP responses (as % of max CAP amplitude in per-drug condition) of injured spinal cord were plotted as pre-drug against 100 μ M 4-AP-3MeOH-treated (C). Original data in C are the same as for B. Overall trends demonstrated a linear relationship between pre-drug and the 4-AP-3 MeOH-treated group. Negligible difference in axon activation thresholds was found after 100 μ M 4-AP-3 MeOH application. $n = 5$. Error bars represent SE.

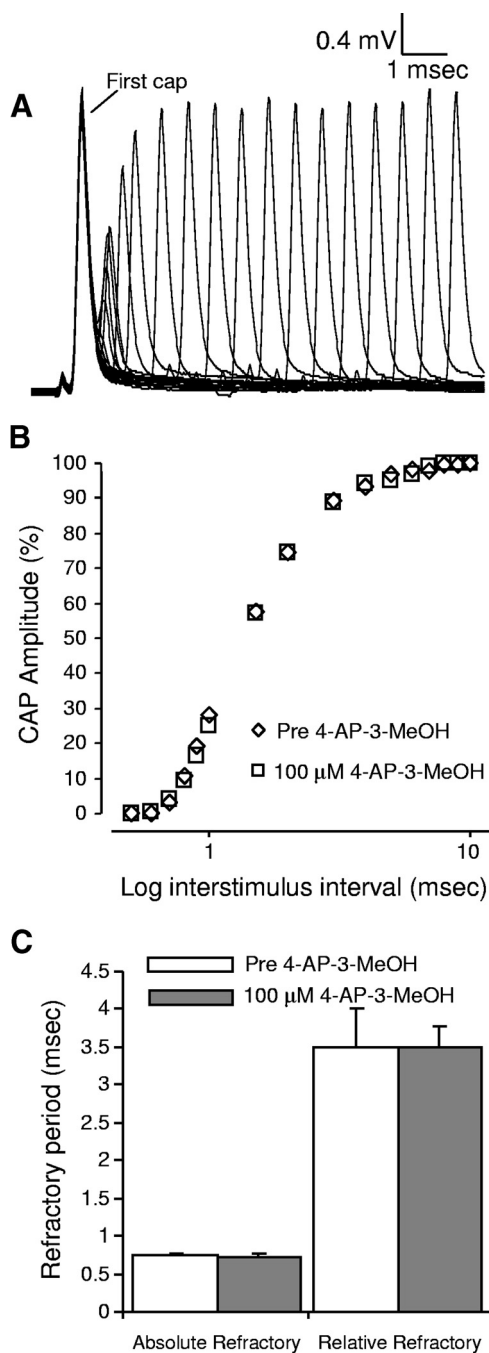


FIG. 5. Dual stimuli with different intervals were applied to injured spinal cord for assessing absolute and relative refractory periods. *A*: individual CAPs superimposed with different intervals between stimuli. The 2nd peak amplitude progressively increased with increased interstimulus intervals. *B*: the 2nd CAP (normalized as a percentage of the 1st CAP) was plotted against log interstimulus interval in pre-drug and 100 μ M 4-AP-3MeOH-treated groups. *C*: little difference between the absolute and relative refractory periods was found in 100 μ M 4-AP-3MeOH-treated samples. The absolute refractory period was defined as the time interval that prior to the appearance of the 2nd CAP. The relative refractory period was defined by the interval time where the 2nd CAP amplitude was no less than 95% of the 1st CAP. $n = 4$. Error bars represent SE.

Following the confirmation of the presence of 4-AP-sensitive fast potassium current, we then tested the ability of 4-AP-3-MeOH to inhibit the same fast potassium currents. Using the same protocol as 4-AP, we have shown that 4-AP-

3-MeOH inhibits the fast potassium currents as well (Fig. 8, *A–C*). Specifically, at +30 mV, 5 mM 4-AP-3-MeOH decreased the fast activated component of potassium currents from $3,501.08 \pm 592.5$ to $2,434.20 \pm 543.4$ pA (Fig. 8, *D* and *E*, $P < 0.05$, $n = 6$, paired *t*-test). In addition to +30 mV, 4-AP-3-MeOH also suppresses I_A at a wide range of step voltage commands from -50 to 40 mV (Fig. 9).

In addition to I_{total} , we also isolated delayed rectifier current I_{dr} , the slow-activated and long sustained component of the potassium current in DRG using a depolarization holding potential (Sun et al. 2009). It was clear that both 4-AP and 4-AP-3-MeOH did not significantly inhibit I_{dr} (data not shown). Thus potassium current that is sensitive to 4-AP and 4-AP-3-MeOH are mostly the fast potassium current I_A .

Stretch injury induces myelin damage at paranodal region and the exposure of voltage-gated potassium channels

The abnormality of myelin structures at the paranodal region were examined using both CARS microscopy and immunohistochemistry. As a novel technique employed in this study, CARS provides excellent resolution in detecting myelin structures, particularly in the node of Ranvier without the need of any exogenous dye labeling (Wang et al. 2005). Figure 10*A* shows the CARS images of nodes of Ranvier in isolated spinal cord ventral white matter under normal conditions and 1.5 h after stretch injury. There is an obvious lengthening or widening of the node of Ranvier that is likely due to the retraction of myelin toward internodal regions. We also noted a weak

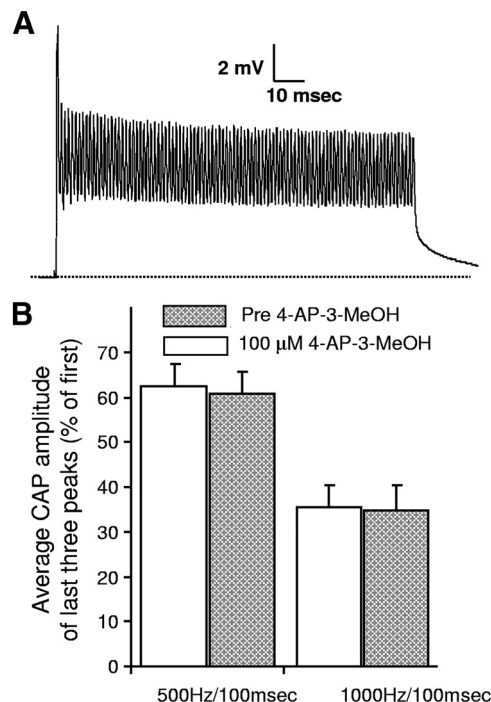


FIG. 6. The CAP response to train stimuli did not change with the treatment of 100 μ M 4-AP-3-MeOH. Train stimuli (100 ms) with high (1,000 Hz) or low (500 Hz) frequency were applied to injured spinal cord strip, respectively. *A*: representative CAP response at 1,000-Hz stimuli. Data shown in *B* represent the averaged amplitudes of the last 4 peaks as a percentage of the 1st peak ($n = 5$). With the treatment of 100 μ M 4-AP-3MeOH, there was no significant differences in the CAP response at both low frequency (500 Hz) and high frequency (1,000 Hz). $n = 5$. Error bars represent SE.

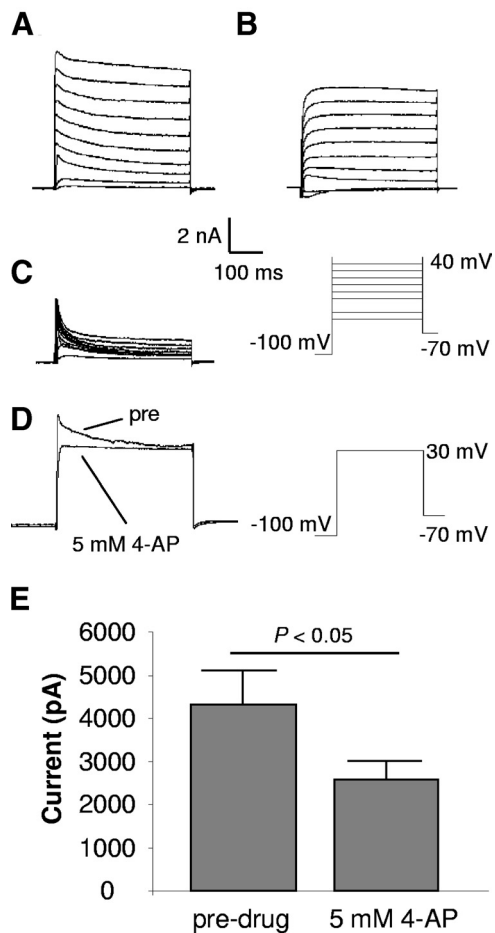


FIG. 7. Potassium current inhibited by 5 mM 4-Aminopyridine treatment. A–C: voltage-gated potassium currents were generated by a series of 400-ms stimuli ranging from -50 to $+40$ mV in 10-mV steps. Holding potential was -70 mV. There was a 2-s prepulse potential held at -100 mV. 4-AP (5 mM) was applied in the bath solution (B). C: the 4-AP-sensitive potassium current by subtracting B from A. For quantification of drug effects, we compared the current amplitude at command potential $+30$ mV in pre- and postdrug conditions. Representative traces are shown in D. The bar graph indicates a decrease in the potassium current from $4,306.38 \pm 810.2$ to $2,574.91 \pm 446.8$ pA ($P < 0.05$, $n = 6$, paired *t*-test) after drug application. Error bars represent SE.

correlation between node ratios and axonal diameter in both control and stretch groups (Fig. 10B). However, there is an obvious increase in the node ratios in the stretched group compared with control group (Fig. 10B). Specifically, the nodal ratio, an indication of nodal lengthening, is increased from a normal level of 0.80 ± 0.1 ($n = 121$) to 2.88 ± 0.2 ($n = 94$; Fig. 10C, $P < 0.01$, Student's *t*-test).

In addition, there is also an obvious paranodal myelin split (or decompaction) in stretched spinal cord strip. Although varying in severity, this splitting or loosening of paranodal myelin can be seen in most of the stretched ventral white matter (Fig. 10A).

It has been reported that there are highly concentrated voltage-gated potassium channels (Kv 1.1, Kv 1.2, Kv β 2.1) in juxtaparade regions on myelinated axons (Poliak and Peles 2003; Rasband and Trimmer 2001; Vabnick and Shrager 1998). We hypothesize that the paranodal demyelination caused by stretch injury will expose those voltage-gated potassium channels. To test such hypothesis, we first examined

the distribution of voltage-gated potassium channels after stretch injury using immunohistology. Specifically, we labeled Kv1.2 channels at 2 h after stretch injury. When observed using both CARS and two photon excitation fluorescence microscopy (TPEF), it is clear that such channels are clustered normally at juxtaparanodal region and covered by myelin. However, stretch-induced paranodal myelin damage clearly exposed the voltage-dependent potassium channels (Fig. 11, D–F).

DISCUSSION

4-AP-3-MeOH enhances CAP conduction after stretch

Using a well-established double sucrose gap recording technique, we have shown in the current study that 4-AP-3-MeOH, a 4-AP derivative, can significantly enhance action potential conductance in guinea pig spinal cord after mechanical stretch. This is the fourth 4-AP derivative in this line of investigation that demonstrates the capability to restore axonal conduction following SCI (McBride et al. 2006, 2007; Smith et al. 2005). Compared with previous three 4-AP derivatives, this com-

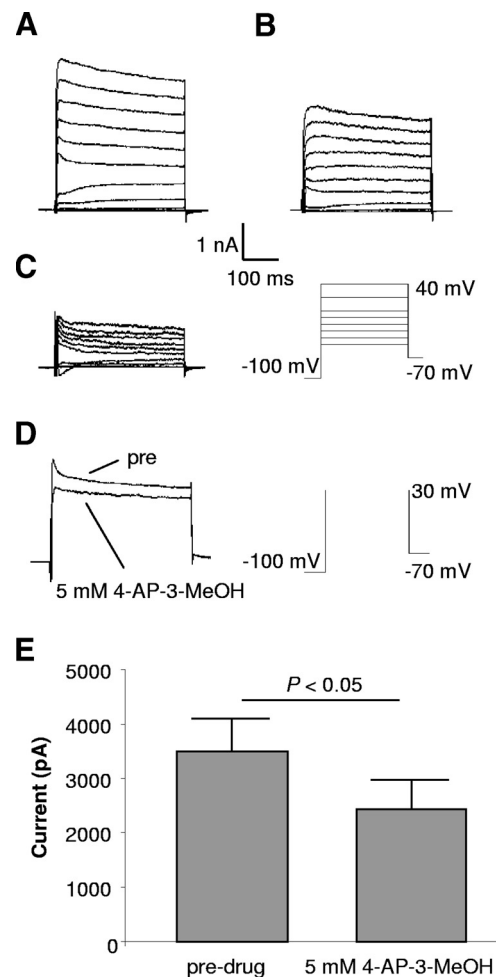


FIG. 8. Potassium current inhibited by 5 mM 4-AP-3-MeOH. A–C: voltage-gated potassium currents were generated with the same protocol described in Fig. 7. C: 4-AP-3-MeOH-sensitive potassium current. For drug effect analysis (D and E), at $+30$ mV, the potassium current dropped from $3,501.08 \pm 592.5$ to $2,434.20 \pm 543.4$ pA ($P < 0.05$, $n = 6$, paired *t*-test). Error bars represent SE.

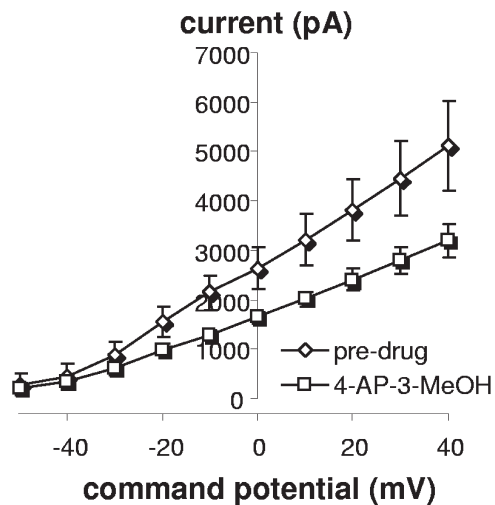


FIG. 9. I - V curve of total potassium currents (I_{total}) recorded from guinea pig dorsal root ganglion (DRG) cells. Potassium currents significantly decreased with 5 mM 4-AP-3-MeOH treatment (\diamond) comparing to pretreatment (\square) record at most command potential levels. Command potentials ranged from -50 to 40 mV with 10 -mV steps. Error bars represent SE. $n = 5$.

pound preserves the advantage of retaining normal electrophysiological properties in restored axonal conduction (McBride et al. 2007). Furthermore, it possesses a unique benefit of being more potent than other three derivatives.

First, 4-AP-3-MeOH showed no preference in restoring in axonal conduction in large or small axons that is similar to previous three derivatives, N -(4-pyridyl)-methyl carbamate, N -(4-pyridyl)-ethyl carbamate, and N -(4-pyridyl)-tertbutyl (Fig. 4) (McBride et al. 2007). Second, in 4-AP-3-MeOH-restored axonal conduction, relative or absolute refractory periods are not significantly altered compared with that of the normal axons (Fig. 5). Similarly, those axons rescued by 4-AP-3-MeOH retained the normal ability to follow repetitive or train stimuli (Fig. 6). It is worth mentioning that while restoring axonal conduction, 4-AP causes significant reduction in axonal responsiveness by increasing the absolute and relative refractory period as well as decreasing the ability of the cord to respond to repetitive stimuli (Jensen and Shi 2003; Targ and Kocsis 1986). In summary, similar to the other three 4-AP derivatives, the axons that are rescued by 4-AP-3-MeOH can conduct action potentials in a manner that is similar to normal axons and superior to those rescued by 4-AP.

Another unique feature of 4-AP-3-MeOH is its high potency compared with other three derivatives and 4-AP: the lowest effective concentration offering conduction enhancement is between 0.01 and $0.1 \mu\text{M}$ (McBride et al. 2006; Shi et al. 1997). This is about a 10 -fold increase of potency compared with other three derivatives and 4-AP (McBride et al. 2006; Shi et al. 1997). Because the side effect of 4-AP is dose related (Shi et al. 1997), it is reasonable to speculate that a lower effective dosage may be accompanied by reduced possibility of inducing serious side effects.

4-AP-3-MeOH inhibits fast potassium current

In the current study, we showed that 4-AP-3-MeOH significantly inhibits an early and transient potassium current in guinea pig DRG cells. Based on its nature of fast activation as well as inactivation, it is likely a fast potassium channel or I_A

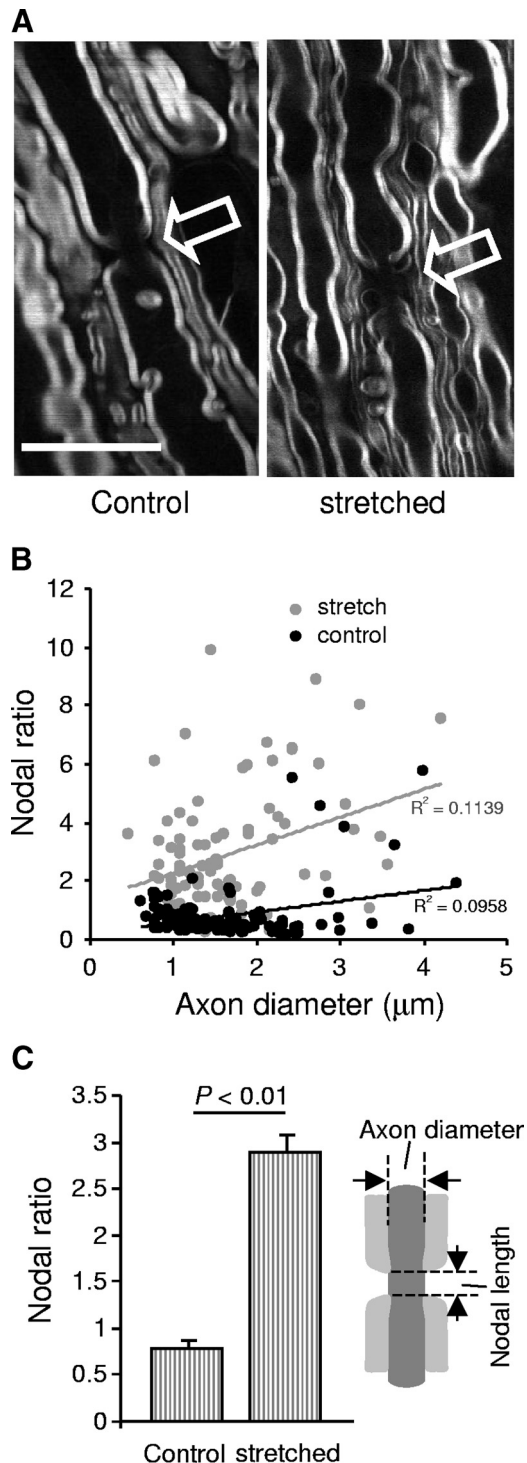


FIG. 10. Stretch-injury-induced paranodal splitting and retraction. **A**: coherent anti-Stokes Raman scattering (CARS) imaging showed paranodal splitting and retraction after acute stretch injury to spinal cord white-matter strip. \leftarrow , node of Ranvier regions. Scale bar: $10 \mu\text{m}$ (for left and right). **B**: node ratios of both control (\bullet) and stretch groups (\odot) were plotted against axonal diameter. Note the weak correlation of nodal ratios and axonal diameters. However, there is a conspicuous increase of node ratios in the stretched group compared with the control group. **C**: comparison of nodal ratio (node length divided by axon diameter, see inset) in control group and stretched group. The nodal ratio was significantly larger in the stretched group (2.88 ± 0.2 , $n = 94$) vs. the control group (0.80 ± 0.1 , $n = 121$; $P < 0.01$, Student's t -test). Error bars represent SE.

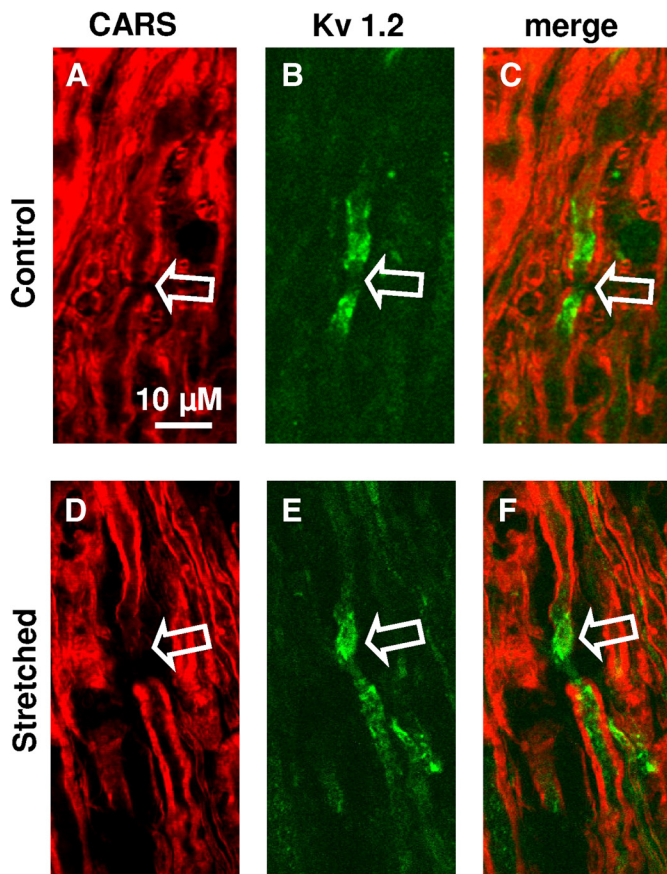


FIG. 11. Stretch injury exposes juxtapanodal Kv1.2 channels. Immunofluorescence labeling of Kv1.2 channels was merged with the myelin signal as revealed by CARS. In normal control spinal cord tissue (A–C), the Kv1.2 channel signal was highly dense in juxtapanodal region and entirely covered by myelin. In stretched tissue (D–F), elongation of node area was obvious, and Kv 1.2 channels were exposed. Scale bar: 10 μm for A–F.

(Sun et al. 2009). This conclusion is further supported by two lines of evidence. First, DRG is known to carry a fast potassium current like I_A (Akins and McCleskey 1993; Everill et al. 1998; Stewart et al. 2003; Tan et al. 2006). Second, 4-AP, a known blocker of I_A , can also inhibit this transient potassium current in the same DRG cells; this further ensures this current is I_A (Sun et al. 2009). Finally, we have also shown recently that another derivative of 4-AP, methyl carbamate can inhibit this transient current, further supporting its identity as I_A (Sun et al. 2009). Therefore it is reasonable to conclude that 4-AP-3-MeOH is indeed an effective blocker of I_A .

In the current study, 4-AP-sensitive current is $\sim 40.2\%$ of the total initial peak of total potassium current (I_{total}), while 30.5% of I_{total} is sensitive to 4-AP-3-MeOH (Figs. 7 and 8). Therefore 4-AP-3-MeOH inhibits $\sim 75\%$ of 4-AP-sensitive K^+ current. This is significantly higher than that of methyl carbamate, which inhibits only 30% of 4-AP-sensitive current (Sun et al. 2009). In conclusion, based on the effects of blocking 4-AP-sensitive current at concentrations of 5 mM, 4-AP-3-MeOH is a more effective blocker than methyl carbamate. This may be contributed to the fact that 4-AP-3-MeOH is 10 times more potent than methyl carbamate.

Based on other literatures and our own experience, the potassium currents recorded in this study should mainly include two components I_A and I_{dr} . However, there is a minor but

noticeable potassium current that is described in this study as well as in a previous paper from this group (Sun et al. 2009) that used the same preparation (DRG cells). This third component of potassium current I_D is fast activated but sustained for a longer period (>400 ms). More importantly, 4-AP-3-MeOH also inhibits this sustained potassium current that is distinct from I_A and I_{dr} yet sensitive to 4-AP and methyl carbamate (Sun et al. 2009). Actually, this sustained current seems to be more prominent in 4-AP-3-MeOH suppressed current than that in 4-AP-suppressed current (Figs. 7 and 8). Therefore 4-AP-3-MeOH seems more effective in inhibiting this third component of I_{total} than was previously described (Everill et al. 1998; Sun et al. 2009). The significance of the inhibition of this third component of potassium current in conduction enhancement in injured axons is not clear. However, considering that 4-AP-3-MeOH is 10 times more potent than other three 4-AP derivatives, including methyl carbamate, in enhancing CAP conduction, it is possible that this third and sustained potassium channel plays a role in conduction loss. Future study using a specific blocker to this sustained current is required to elucidate such a hypothesis.

Stretch injury results in the exposure of potassium channel at juxtapanodal region

It has long been suggested that mechanical injury causes myelin disruption as well as subsequent axonal conduction failure in mammalian spinal cord (Blight and DeCrescito 1986; Bunge et al. 1960; Cao et al. 2005). However, the detailed mechanisms of demyelination-induced axonal conduction failure have not been well established. In mammalian myelinated axons, proper paranodal myelin structure is crucial for the generation and propagation of action potentials by restricting the potassium channels under the myelin (Poliak and Peles 2003). The exposure of such potassium channels as a result of injury is thought to short circuit depolarization and derails the genesis of action potentials, leading to conduction failure (Blight 1989; Jensen and Shi 2003; Shi et al. 1997). However, the evidence supporting the exposure of voltage-dependent potassium channels was still circumstantial. For example, Fehlings and his colleagues have shown the abnormal distribution of potassium channels after mechanical injury (Karimi-Abdolrezaee et al. 2004; Nashmi et al. 2000). However, because the myelin was not imaged at the same time, it is uncertain regarding the relationship between the myelin and the underlying potassium channels at the juxtapanodal region. This is particularly true in acute spinal cord trauma when the myelin damage begins to emerge (Karimi-Abdolrezaee et al. 2004).

In the current study, using a combination of traditional and novel multimodal imaging techniques (CARS and 2-photon excitation fluorescence microscopy), we have provided unequivocal anatomical evidence demonstrating the exposure of potassium channels after mechanical insult in guinea pig spinal cord. With myelin imaged by CARS (without any labeling) and potassium channels imaged by fluorescence microscopy, we revealed the exposure of potassium channels in reference to the myelin for the first time. This is particularly significant in demonstrating the partial exposure of potassium channels that may not be clear using other methods (Howell et al. 2006; Karimi-Abdolrezaee et al. 2004; Nashmi et al. 2000). This is certainly consistent and further confirmation of the previous

hypothesis and observation under similar situations (Karimi-Abdolrezaee et al. 2004; Nashmi et al. 2000).

In summary, we have demonstrated the ability of 4-AP-3-MeOH, a 4-aminopyridine derivative, to significantly restore axonal conduction and act as an effective I_A blocker. This compound has the advantage of being 10 times more potent when compared with 4-AP and other derivatives. Furthermore, unlike 4-AP, 4-AP-3-MeOH can restore axonal conduction without changing their electrophysiological properties. We have also provided the critical evidence to confirm the exposure of potassium channels after mechanical injury. Taken together, our data further support the role of potassium channels in conduction loss and its therapeutic value as an effective target for intervention. Furthermore, due to its high potency and low side effects impacting electrophysiological properties, 4-AP-3-MeOH has the potential to be developed as an important agent in reversing conduction block in SCI.

ACKNOWLEDGMENTS

We thank S. Connell and Dr. Jianming Li for critically reading the manuscript.

GRANTS

The authors acknowledge financial support from the Purdue Research Foundation to D. Smith and R. Shi.

REFERENCES

- Akins PT, McCleskey EW.** Characterization of potassium currents in adult rat sensory neurons and modulation by opioids and cyclic AMP. *Neuroscience* 56: 759–769, 1993.
- Blight AR.** Axonal physiology of chronic spinal cord injury in the cat: intracellular recording in vitro. *Neuroscience* 10: 1471–1486, 1983a.
- Blight AR.** Cellular morphology of chronic spinal cord injury in the cat: analysis of myelinated axons by line-sampling. *Neuroscience* 10: 521–543, 1983b.
- Blight AR.** Effect of 4-aminopyridine on axonal conduction-block in chronic spinal cord injury. *Brain Res Bull* 22: 47–52, 1989.
- Blight AR, DeCrescito V.** Morphometric analysis of experimental spinal cord injury in the cat: the relation of injury intensity to survival of myelinated axons. *Neuroscience* 19: 321–341, 1986.
- Blight AR, Gruner JA.** Augmentation by 4-aminopyridine of vestibulospinal free fall responses in chronic spinal-injured cats. *J Neurol Sci* 82: 145–159, 1987.
- Blight AR, Toombs JP, Bauer MS, Widmer WR.** The effects of 4-aminopyridine on neurological deficits in chronic cases of traumatic spinal cord injury in dogs: a phase I clinical trial. *J Neurotrauma* 8: 103–119, 1991.
- Bunge RP, Bunge MB, Ris H.** Electron microscopic study of demyelination in an experimentally induced lesion in adult cat spinal cord. *J Biophys Biochem Cytol* 7: 685–696, 1960.
- Cao Q, Zhang YP, Iannotti C, DeVries WH, Xu XM, Shields CB, Whittemore SR.** Functional and electrophysiological changes after graded traumatic spinal cord injury in adult rat. *Exp Neurol* 191 Suppl 1: S3–S16, 2005.
- Donovan WH, Halter JA, Graves DE, Blight AR, Calvillo O, McCann MT, Sherwood AM, Castillo T, Parsons KC, Strayer JR.** Intravenous infusion of 4-AP in chronic spinal cord injured subjects. *Spinal Cord* 38: 7–15, 2000.
- Everill B, Rizzo MA, Kocsis JD.** Morphologically identified cutaneous afferent DRG neurons express three different potassium currents in varying proportions. *J Neurophysiol* 79: 1814–1824, 1998.
- Fu Y, Wang H, Huff TB, Shi R, Cheng JX.** Coherent anti-Stokes Raman scattering imaging of myelin degradation reveals a calcium-dependent pathway in lyso-PtdCho-induced demyelination. *J Neurosci Res* 85: 2870–2881, 2007.
- Fujihara K, Miyoshi T.** The effects of 4-aminopyridine on motor evoked potentials in multiple sclerosis. *J Neurol Sci* 159: 102–106, 1998.
- Haghighi SS, Pugh SL, Perezespejo MA, Oro JJ.** Effect of 4-aminopyridine in acute spinal cord injury. *Surg Neurol* 43: 443–447, 1995.
- Halter JA, Blight AR, Donovan WH, Calvillo O.** Intrathecal administration of 4-aminopyridine in chronic spinal injured patients. *Spinal Cord* 38: 728–732, 2000.
- Hansebout RR, Blight AR, Fawcett S, Reddy K.** 4-aminopyridine in chronic spinal cord injury: a controlled, double-blind, crossover study in eight patients. *J Neurotrauma* 10: 1–18, 1993.
- Hayes K, C, Hsieh JTC, Potter PJ, Wolfe DL, Delaney GA, Blight AB.** Effects of induced hypothermia on somatosensory evoked potentials in patients with chronic spinal cord injury. *Paraplegia* 31: 730–741, 1993.
- Hayes KC, Potter PJ, Wolfe DL, Hsieh JTC, Delaney GA, Blight AR.** 4-Aminopyridine-sensitive neurologic deficits in patients with spinal cord injury. *J Neurotrauma* 11: 433–446, 1994.
- Hayes KC, Kakulas BA.** Neuropathology of human spinal cord injury sustained in sports-related activities. *J Neurotrauma* 14: 235–248, 1997.
- Howell OW, Palsler A, Polito A, Melrose S, Zonta B, Scheiermann C, Vora AJ, Brophy PJ, Reynolds R.** Disruption of neurofascin localization reveals early changes preceding demyelination and remyelination in multiple sclerosis. *Brain* 129: 3173–3185, 2006.
- Jensen JM, Shi R.** Effects of 4-aminopyridine on stretched mammalian spinal cord: the role of potassium channels in axonal conduction. *J Neurophysiol* 90: 2334–2340, 2003.
- Jones RE, Heron JR, Foster DH, Snelgar RS, Mason RJ.** Effects of 4-aminopyridine in patients with multiple sclerosis. *J Neurol Sci* 60: 353–362, 1983.
- Kakulas BA.** A review of the neuropathology of human spinal cord injury with emphasis on special features. *J Spinal Cord Med* 22: 119–124, 1999.
- Karimi-Abdolrezaee S, Eftekharpour E, Fehlings MG.** Temporal and spatial patterns of Kv1.1 and Kv1.2 protein and gene expression in spinal cord white matter after acute and chronic spinal cord injury in rats: implications for axonal pathophysiology after neurotrauma. *Eur J Neurosci* 19: 577–589, 2004.
- McBride JM, Smith DT, Byrn SR, Borgens RB, Shi R.** Dose responses of three 4-aminopyridine derivatives on axonal conduction in spinal cord trauma. *Eur J Pharm Sci* 27: 237–242, 2006.
- McBride JM, Smith DT, Byrn SR, Borgens RB, Shi R.** 4-Aminopyridine derivatives enhance impulse conduction in guinea-pig spinal cord following traumatic injury. *Neuroscience* 148: 44–52, 2007.
- Nashmi R, Jones OT, Fehlings MG.** Abnormal axonal physiology is associated with altered expression and distribution of Kv1.1 and Kv1.2 K⁺ channels after chronic spinal cord injury. *Eur J Neurosci* 12: 491–506, 2000.
- Pena F, Tapia R.** Relationships among seizures, extracellular amino acid changes, and neurodegeneration induced by 4-aminopyridine in rat hippocampus: a microdialysis and electroencephalographic study. *J Neurochem* 72: 2006–2014, 1999.
- Pena F, Tapia R.** Seizures and neurodegeneration induced by 4-aminopyridine in rat hippocampus in vivo: role of glutamate- and GABA-mediated neurotransmission and of ion channels. *Neuroscience* 101: 547–561, 2000.
- Poliak S, Peles E.** The local differentiation of myelinated axons at nodes of Ranvier. *Nat Rev Neurosci* 4: 968–980, 2003.
- Rasband MN, Trimmer JS.** Developmental clustering of ion channels at and near the node of Ranvier. *Dev Biol* 236: 5–16, 2001.
- Shi R, Asano T, Vining NC, Blight AR.** Control of membrane sealing in injured mammalian spinal cord axons. *J Neurophysiol* 84: 1763–1769, 2000.
- Shi R, Blight AR.** Compression injury of mammalian spinal cord in vitro and the dynamics of action potential conduction failure. *J Neurophysiol* 76: 1572–1580, 1996.
- Shi R, Blight AR.** Differential effects of low and high concentrations of 4-aminopyridine on axonal conduction in normal and injured spinal cord. *Neuroscience* 77: 553–562, 1997.
- Shi R, Borgens RB.** Acute repair of crushed guinea pig spinal cord by polyethylene glycol. *J Neurophysiol* 81: 2406–2414, 1999.
- Shi R, Kelly TM, Blight AR.** Conduction block in acute and chronic spinal cord injury: Different dose-response characteristics for reversal by 4-aminopyridine. *Exp Neurol* 148: 495–501, 1997.
- Shi R, Pryor JD.** Temperature dependence of membrane sealing following transection in mammalian spinal cord axons. *Neuroscience* 98: 157–166, 2000.
- Shi R, Pryor JD.** Pathological changes of isolated spinal cord axons in response to mechanical stretch. *Neuroscience* 110: 765–777, 2002.
- Shi R, Whitebone J.** Conduction deficits and membrane disruption of spinal cord axons as a function of magnitude and rate of strain. *J Neurophysiol* 95: 3384–3390, 2006.
- Smith DT, Shi R, Borgens RB, McBride JM, Jackson K, Byrn SR.** Development of novel 4-aminopyridine derivatives as potential treatments for neurological injury and disease. *Eur J Med Chem* 40: 908–917, 2005.
- Stefoski D, Davis FA, Faut M, Schauf CL.** 4-Aminopyridine improves clinical signs in multiple sclerosis. *Ann Neurol* 21: 71–77, 1987.

- Stewart T, Beyak MJ, Vanner S.** Iletis modulates potassium and sodium currents in guinea pig dorsal root ganglia sensory neurons. *J Physiol* 552: 797–807, 2003.
- Stork CM, Hoffman RS.** Characterization of 4-aminopyridine in overdose. *J Toxicol Clin Toxicol* 32: 583–587, 1994.
- Sun W, Smith D, Bryn S, Borgens R, Shi R.** *N*-(4-pyridyl) methyl carbamate inhibits fast potassium currents in guinea pig dorsal root ganglion cells. *J Neurol Sci* 277: 114–118, 2009.
- Tan ZY, Donnelly DF, LaMotte RH.** Effects of a chronic compression of the dorsal root ganglion on voltage-gated Na⁺ and K⁺ currents in cutaneous afferent neurons. *J Neurophysiol* 95: 1115–1123, 2006.
- Targ EF, Kocsis JD.** Action potential characteristics of demyelinated rat sciatic nerve following application of 4-aminopyridine. *Brain Res* 363: 1–9, 1986.
- Vabnick I, Shrager P.** Ion channel redistribution and function during development of the myelinated axon. *J Neurobiol* 37: 80–96, 1998.
- Wang H, Fu Y, Zickmund P, Shi R, Cheng JX.** Coherent anti-stokes Raman scattering imaging of axonal myelin in live spinal tissues. *Biophys J* 89: 581–591, 2005.
- Waxman SG.** Demyelination in spinal cord injury. *J Neurol Sci* 91: 1–14, 1989.
- Waxman SG.** Demyelination in spinal cord injury and multiple sclerosis: what can we do to enhance functional recovery? *J Neurotrauma* 9: S105–S117, 1992.
- Waxman SG, Utzschneider DA, Kocsis JD.** Enhancement of action potential conduction following demyelination: experimental approaches to restoration of function in multiple sclerosis and spinal cord injury. *Prog Brain Res* 100: 233–243, 1994.
- Xu GY, Winston JH, Shenoy M, Yin H, Pasricha PJ.** Enhanced excitability and suppression of A-type K⁺ current of pancreas-specific afferent neurons in a rat model of chronic pancreatitis. *Am J Physiol Gastrointest Liver Physiol* 291: G424–431, 2006.